

## ORIGINAL RESEARCH

# Cellular tropism of SARS-CoV-2 in various organs- A Histopathology and Immunohistochemistry study on Covid-19 Deaths

<sup>1</sup>Dr. Nirmala C, <sup>2</sup>Dr. Ashwini B R, <sup>3</sup>Dr. Dayananda S Biligi, <sup>4</sup>Dr. Ravi N

<sup>1</sup>Professor, <sup>2</sup>Assistant Professor, <sup>3</sup>Professor and Head, Department of Pathology, BMCRI, Bengaluru, Karnataka, India

<sup>4</sup>Professor, Department of Radiology, BMCRI, Bengaluru, Karnataka, India

### Corresponding Author

Dr. Nirmala C

Professor, Department of Pathology, BMCRI, Bengaluru, Karnataka, India

Received: 13 February, 2023

Accepted: 16 March, 2023

### ABSTRACT

**Background and objectives:** SARS-CoV-2 infections have varied manifestations among individuals ranging from asymptomatic or mild symptoms to severe disease and death. This study is done to look into various histopathological changes in lung, liver, and kidney tissues among Covid19 positive autopsies with cellular tropism and viral load among various organs by immunohistochemistry (IHC) for the SARS-CoV-2 viral marker. **Methods:** A prospective descriptive study of core biopsies from covid19 positive autopsies from the lung, liver, and kidneys were taken from 20 cases. A routine histopathological examination of the tissues with IHC staining for SARS-CoV-2 cocktail antibodies was performed and assessed. **Results:** Histopathological changes in the lung, liver, and kidney tissues showed changes of varying severity. On IHC, in the lung, the tropism for SARS-CoV-2 was seen in pneumocytes, bronchial epithelial cells, endothelial cells, and macrophages. In the kidney, tropism was seen towards tubular epithelial cells and endothelial cells. In the liver, hepatocytes and bile duct epithelial cells were positive. Variable viral density was seen in different organs which varied from case to case. The density of the viral load was highest in the lung and lower in the kidney and least in the liver. **Conclusion:** In this study the various histopathological changes and cellular tropism of the SARS-CoV-2 among Lung, liver, and kidney tissues have been described and compared with various similar studies across the globe.

**Keywords:** Cellular Tropism, Covid-19 Autopsies, Histopathology, Immunohistochemistry, Kidney, Liver, Lung, SARS-CoV-2

---

This is an open access journal, and articles are distributed under the terms of the Creative Commons Attribution-Non Commercial-Share Alike 4.0 License, which allows others to remix, tweak, and build upon the work non-commercially, as long as appropriate credit is given and the new creations are licensed under the identical terms.

---

### INTRODUCTION

The COVID-19 pandemic caused by the Severe Acute Respiratory Distress Syndrome-Coronavirus 2 (SARS-CoV-2) has made a great impact on the lives of every individual young and old across the globe. Answers to the questions about the disease, pathology, and pathogenesis in various organs need to be addressed. Observing the histopathological changes in various organs and localizing the viral particles by Immunohistochemistry (IHC), studying the cellular tropism will help us a better understanding of the pathogenesis of Covid 19 infection. This insight would aid in the better management of the affected patients. With this aim, we planned to study the

various histopathological features and IHC for viral particles in lungs, liver, and kidney tissues of Covid19 deaths at our institution.

### MATERIALS AND METHODS

A prospective descriptive study with core biopsies of lungs, liver, and kidneys was done in 20 cases of deaths due to SARS-CoV-2 viral infections. This study was conducted for a period of 3 months from December 2020 to February 2021 after obtaining ethical committee clearance from the institution. Written informed consent was obtained from the deceased relatives. Within 6 hrs after the death of the individual due to COVID-19, a core needle biopsy was performed using an 18g core biopsy gun under

ultrasound guidance. All the universal precautions against SARS-CoV-2 infection were followed during the procedure.

Five biopsies were taken from each autopsy case which included one biopsy from each lung, one from the liver, and one each from the right and left kidneys. The biopsy material was fixed in 10% buffered formalin for 48 hrs followed by histopathological processing. Following routine processing 2 to 3 sections of 4 μ thickness were cut from each core and stained with hematoxylin and eosin (H&E) stain. The histopathological findings were then recorded and other clinical findings were collected from the hospital records. The data was then statistically analyzed using descriptive statistics.

IHC was performed on additional sections in 10/20 cases. IHC staining was done on Formalin fixed paraffin embedded (FFPE) block with 5-micron thick sections. Antigen retrieval was done with phosphate buffer at PH 9. Primary antibody of SARS-CoV-2 of mouse monoclonal antibody of Biorbyt, UK was used. A coronavirus cocktail antibody of dilution 1:100 was used. The secondary antibody was from Path-in-situ company. 0.05 molar tris buffer wash solution of PH 7.6 was used in the IHC procedure.

**RESULTS:**

A total of 20 autopsy cases were studied by collecting the core biopsies. All the patients had tested SARS-CoV-2 positive by Real Time Polymerase chain reaction (RT-PCR). The age of the deceased in our study ranged from 18 years to 88 years. More males were affected than females in our study with a male-to-female ratio of 2.3: 1.

Co-morbidities like Diabetes were noted in 17 cases (85%), Hypertension in 10 cases (50%), chronic kidney disease in 4 cases (20%), obesity in 2 cases (10%), carcinoma colon in 1 case, and sepsis in 1 case. Many patients with Covid 19 had multiple co-morbidities. However, in one case an 18-year-old male had no co-morbidities but showed extensive micro-thrombi and haemorrhage in the organs studied.

**Histopathological features and Immunohistochemistry of various organs:**

The Hematoxylin and Eosin (H&E) stained slides of core biopsies were studied in 20 cases and the various histopathological changes are as shown in **table 1**. The IHC staining was performed on 10 cases with features as shown in **table 2**.

**Table1: Shows histopathological features among different organs affected with SARS-CoV-2**

Findings	No of cases with %
<b>LUNGS</b>	
Hyaline membrane	12 cases (60%)
reactive atypical pneumocytes	14 cases (70%)
pneumocyte hyperplasia	10 cases (50%)
interstitial odema	7 cases (35%)
interstitial fibroblastic proliferation	13 cases (65%)
Angiogenesis	13 cases (65%)
interstitial fibrosis	8 cases (40%)
architectural remodelling fibrosis	7 cases (35%)
Squamous metaplasia	4 cases (20%).
<b>KIDNEYS</b>	
Diabetic glomerulosclerosis	4 cases (20%)
Glomerular microthrombopathy	7 cases (35%)
hyaline arteriolosclerosis	1 case (5%)
chronic pyelonephritis	7 cases (35%)
Acute tubular epithelial cell damage	18 cases (90%)
Acute tubular epithelial cell detachment	17 cases (85%)
fibrin microthrombi	15 cases (75%)
<b>LIVER</b>	
Interstitial congestion	10 cases (50%)
Hemorrhage	4 cases (20%)
microvesicularsteatosis	15 cases (75%)
regeneration	13 cases (65%)
single cell necrosis	3 cases (15%)
cytopathic changes	10 Cases (50%)
Sinusidal congestion	13 cases (65%)
Portal area- lymphocytic inflammation	19 cases (95%)
Lobular inflammation	8 cases (40%)

Intensity of staining	3+	2+	1+	0
<b>Lungs</b>				
Pneumocytes	3(30%)	4(40%)	3(30%)	0
Hyaline membrane	4(40%)	3(30%)	2(20%)	1(10%)
Endothelial cell	1(10%)	0	3(30%)	6(60%)
Fibroblast	0	0	3(30%)	7(70%)
Bronchial Epithelial cell	0	1(10%)	1(10%)	0
<b>Kidneys</b>				
Tubular epithelial cell	4(40%)	2(20%)	1(10%)	3(30%)
Endothelial cell	0	2(20%)	2(20%)	6(60%)
<b>Liver</b>				
Hepatocytes	0	2 (20%)	2 (20%)	6 (60%)
Bile duct epithelial cells	0	0	1 (10%)	9 (90%)

**Table 2-** shows intensity of staining by IHC in various cells affected by SARS-CoV-2.

### Histopathological Changes of Lungs:

The histopathological examination of the lungs showed evidence of diffuse alveolar damage (DAD) in 19 cases (95%). Both the exudative phase and proliferative phase of DAD were observed in our cases. A few cases showed overlapping features of both phases.

The exudative phase of DAD was seen in 14 cases (70%) which were characterized by the presence of a hyaline membrane within the alveoli, reactive atypical pneumocytes, hyperplasia of pneumocytes, and interstitial edema. Reactive atypical pneumocytes were characterized by enlarged cuboidal to oval alveolar lining epithelial cells with enlarged hyperchromatic nuclei, prominent nucleoli, and abundant eosinophilic cytoplasm. Focally hyperplasia and of these pneumocytes were noted. The hyaline membrane characterized by thick homogenous eosinophilic material was seen cementing the alveolar wall with inflammatory exudate and detached pneumocytes in the alveolar lumen.

The proliferative phase of DAD was seen in 13 cases (65%), characterized by interstitial fibroblastic proliferation and angiogenesis. The fibroblasts appeared spindle to stellate shaped and were arranged haphazardly surrounded by fine collagen both in the alveolar septae and within the alveolar lumen causing thickening of the alveolar septae. Prominent angiogenesis was noted in this phase with endothelial proliferation in the septa with many of the endothelial cells showing intracytoplasmic lumen formation. These cells were seen in tufts and also were disorderly arranged amidst the proliferating fibroblasts.

The chronic phase of DAD was seen in 8 cases (40%) characterized by interstitial fibrosis and architectural remodeling. The absence of alveolar lining epithelium was noted with fibroblastic proliferation, dense collagen deposition within the septae, and an increase in angiogenesis in this phase.

Squamous metaplasia of the alveolar lining epithelium was seen in a few cases in this stage.

Two cases showed vascular microthrombi in the small septal vessels of the lung tissue. Mild inflammation of the lung parenchyma was seen in 14 cases (70%) with lymphocytes in 12 cases (60%), neutrophils in 5 cases, and occasional mast cells in 2 cases. The inflammatory infiltrate was predominantly noted in the alveolar septae with occasional cases showing inflammatory cells within the lumen along with alveolar macrophages.

Acute Fibrinous organizing pneumonia (AFOP) characterized by the presence of fibrin in the alveolar lumen along with sparse inflammatory cells was seen in 4 cases (20%). The histopathological features of lungs are as seen in figure 1, figure 2, figure 3 and figure 4.

### Immunohistochemistry Changes of Lungs

Immunostaining of the lung tissue in 10 cases with the SARS-CoV-2 viral cocktail antibodies revealed the presence of viral particles as extracellular and intracellular particles. The lung tissue showed positivity in all 10 cases (100%) with the pneumocytes being positive in all the cases. Most intense staining was observed in the pneumocytes seen lining the alveoli and as detached pneumocytes in the alveolar lumen.

Extracellular viral particles were seen in the alveolar exudates, and the hyaline membrane lining the alveoli was positive in 90% of the cases. Bronchial lining epithelial cells also showed the presence of viral particles in 2 (20%) cases. Endothelial cells and the blood showed rare particles in 4(40%) cases. The intensity of staining of viral particles was observed to be varied with cases and the various types of cells. The intensity of staining was found to be higher in the pneumocytes(3+ in 30%) and hyaline membrane (3+ in 40%) as compared to the endothelial cells and fibroblasts in the lung tissue.

The intensity of staining with viral particles was more intense in the early acute exudative phase compared to the cases in the late organizing phase with interstitial fibrosis where the intensity of staining was mild suggesting the presence of few viral particles. The Immunohistochemistry changes in lungs are as shown in figure 5.

#### **Histopathological Changes Of Kidneys**

Kidneys showed evidence of chronic kidney disease with diabetic glomerulosclerosis in 20% of cases, Hypertensive changes including hyaline arteriolosclerosis and chronic pyelonephritis were also seen in 5% and 20% of cases respectively.

Acute tubular epithelial cell damage was one of the prominent findings in the kidneys seen in 90% of cases. Enlargement of tubular epithelial cells, increased eosinophilia, loss of nuclei, detachment of tubular epithelial cells, and disruption of the basement membrane were seen in these cases. The vascular fibrin microthrombi within the small capillary blood vessels were noted in 75% of cases.

#### **Immunohistochemistry Changes of Kidney:**

Tissue showed positivity for the viral marker in 7 of 10 cases. Kidney tissue showed positivity for the viral marker in tubular epithelial cells in 70% of cases, and endothelial cells in 50 % of cases. The intensity of staining varied with cells with higher intensity in the tubular epithelial cells. The number of endothelial cells and the intensity of staining were lower.

The histopathological features and IHC of viral particles in Kidney are as seen in figure 6.

#### **Histopathological Changes Of The Liver**

The hepatocytes showed varying degrees of hepatocellular damage seen predominantly in the centrilobular region ranging from ballooning degeneration of hepatocytes to hemorrhagic necrosis. Acute liver damage characterized by centrilobular necrosis was seen in 7 cases (35%). The hepatocytes also showed features of microvesicular steatosis, regeneration, single cell necrosis, and viral cytopathic changes with enlarged nuclei showing ground glass appearance in all three zones of the hepatic acini. Sinusoidal congestion was noted in 13 cases (65%). Portal inflammation with lymphocytes was seen in 95% of the cases. Mild lobular inflammation was seen in 8 cases (40%) with lymphocytes and neutrophils in 6 and 2 cases respectively.

#### **Immunohistochemistry Changes of Liver**

The liver showed positivity for the viral marker in 4 cases. Hepatocytes were seen more commonly to show with viral markers and were seen in 40% of cases, bile duct epithelium was found positive in one case. The intensity of staining was seen higher in hepatocytes in number as well as intensity as compared to the bile duct epithelium positivity was seen in only one case of mild intensity. The histopathological features and IHC of viral particles in liver are as seen in figure 7 and figure 8 respectively.

Intra nuclear inclusions were seen in hepatocytes affected by SRS Co-V 2 infection as seen in figure 9.

**Figure 1: Shows Histopathological changes of lung affected by SARS CoV2 infection, showing overlapping exudative and proliferative phase. H&E ,10X.**

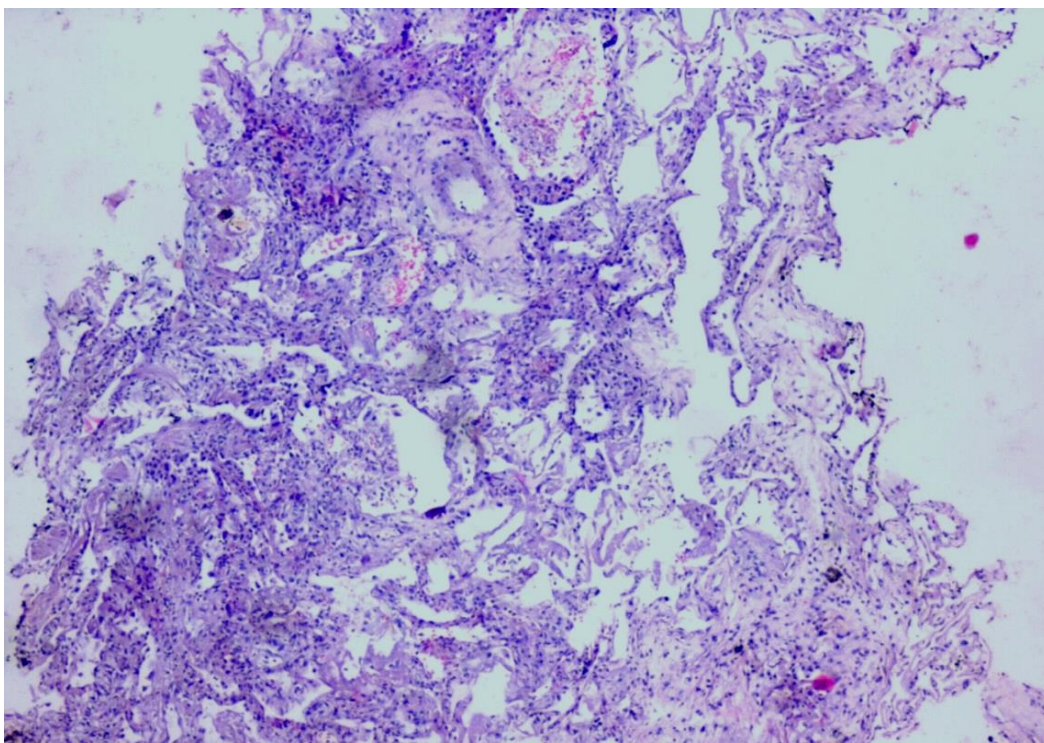


**Fig 2 - Lung tissue with alveolar wall with evidence of endothelial and fibroblastic proliferation. H&E, 20X.**

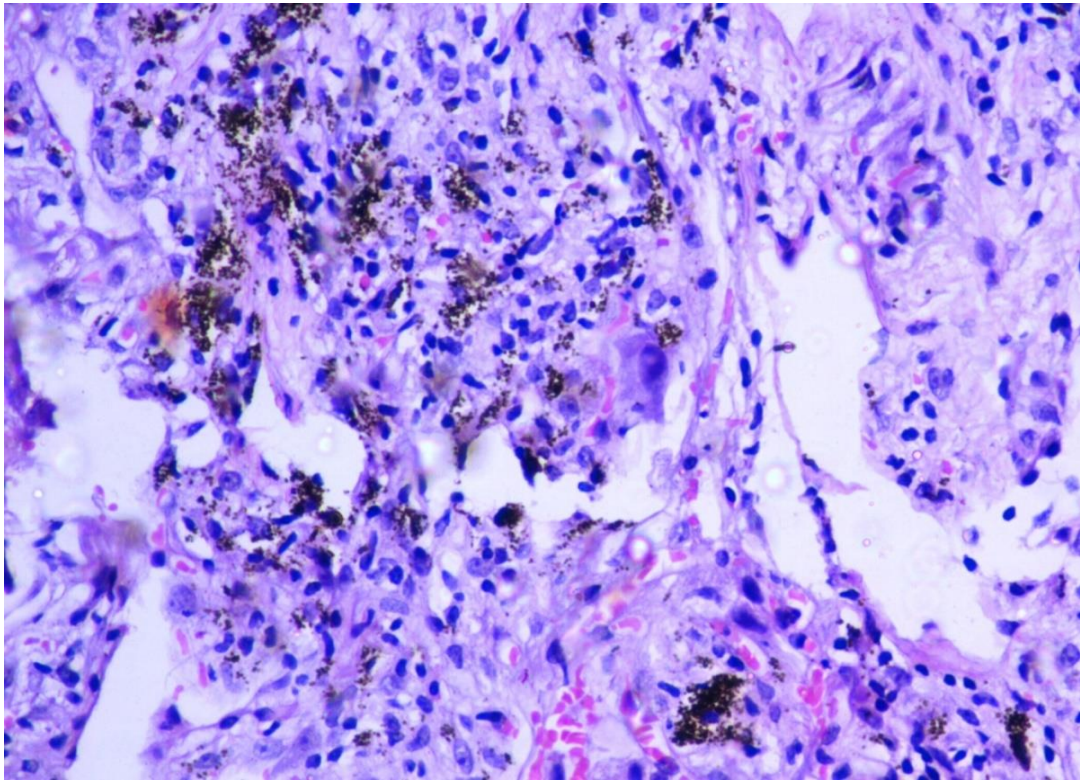


**Figure 3: Lung tissue with vascular microthrombi . H&E ,40X.**

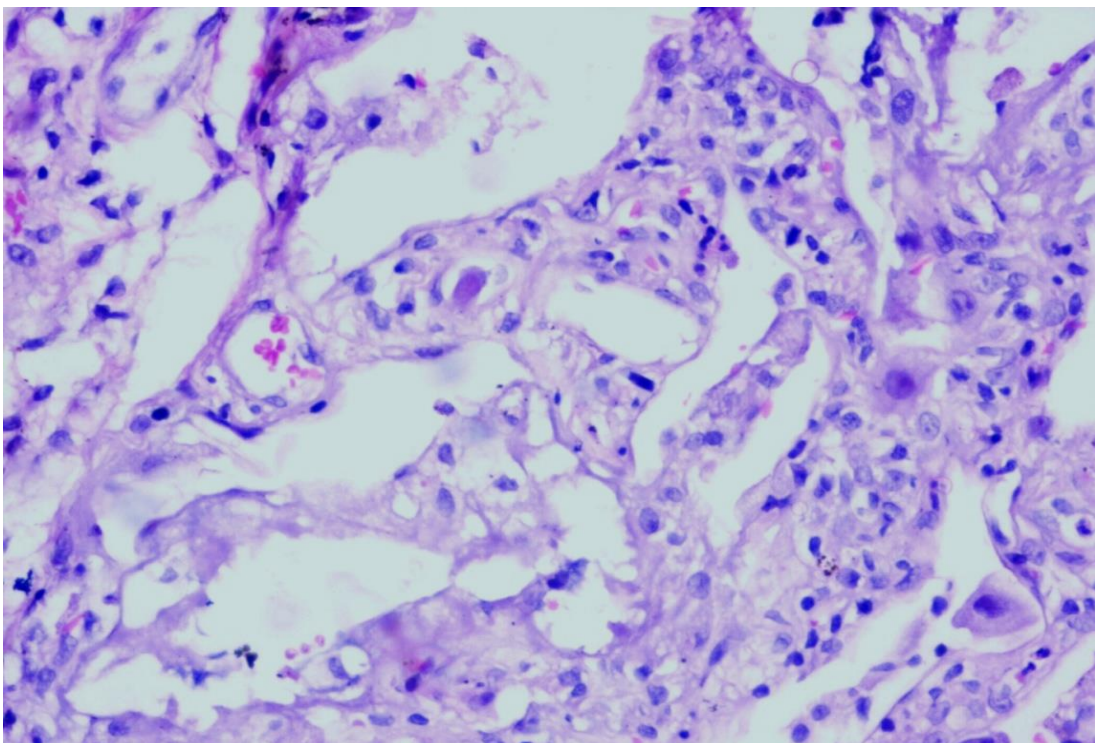


**Figure 4: Lung tissue with alveolar wall with evidence of endothelial proliferation. H&E, 40X.**

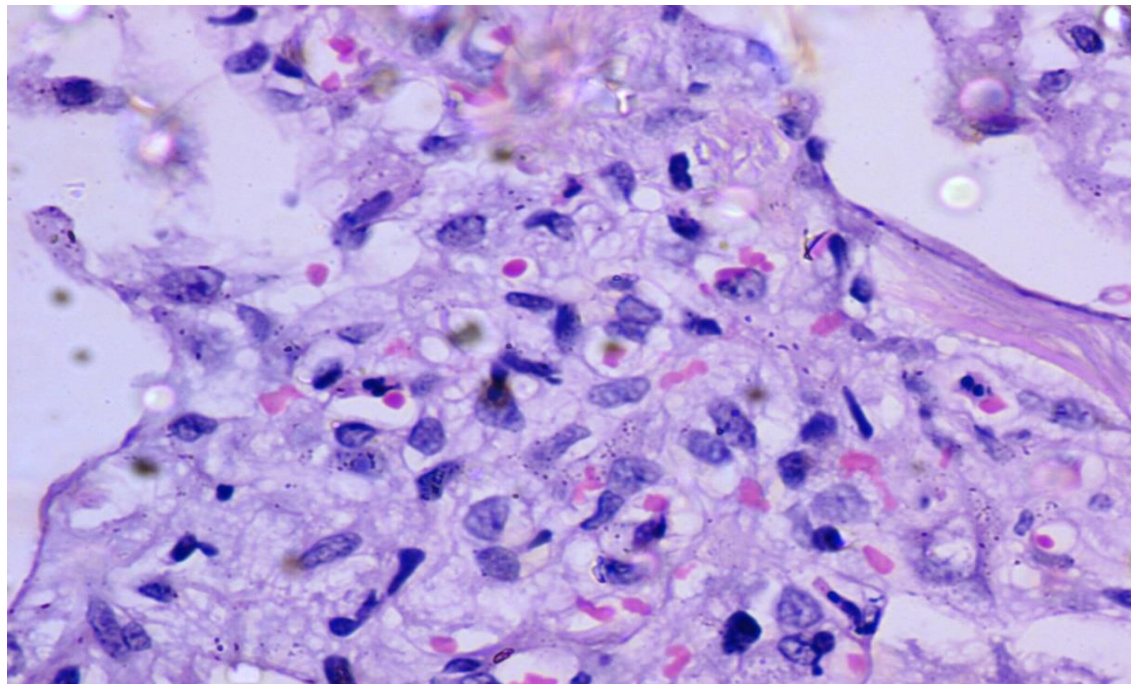
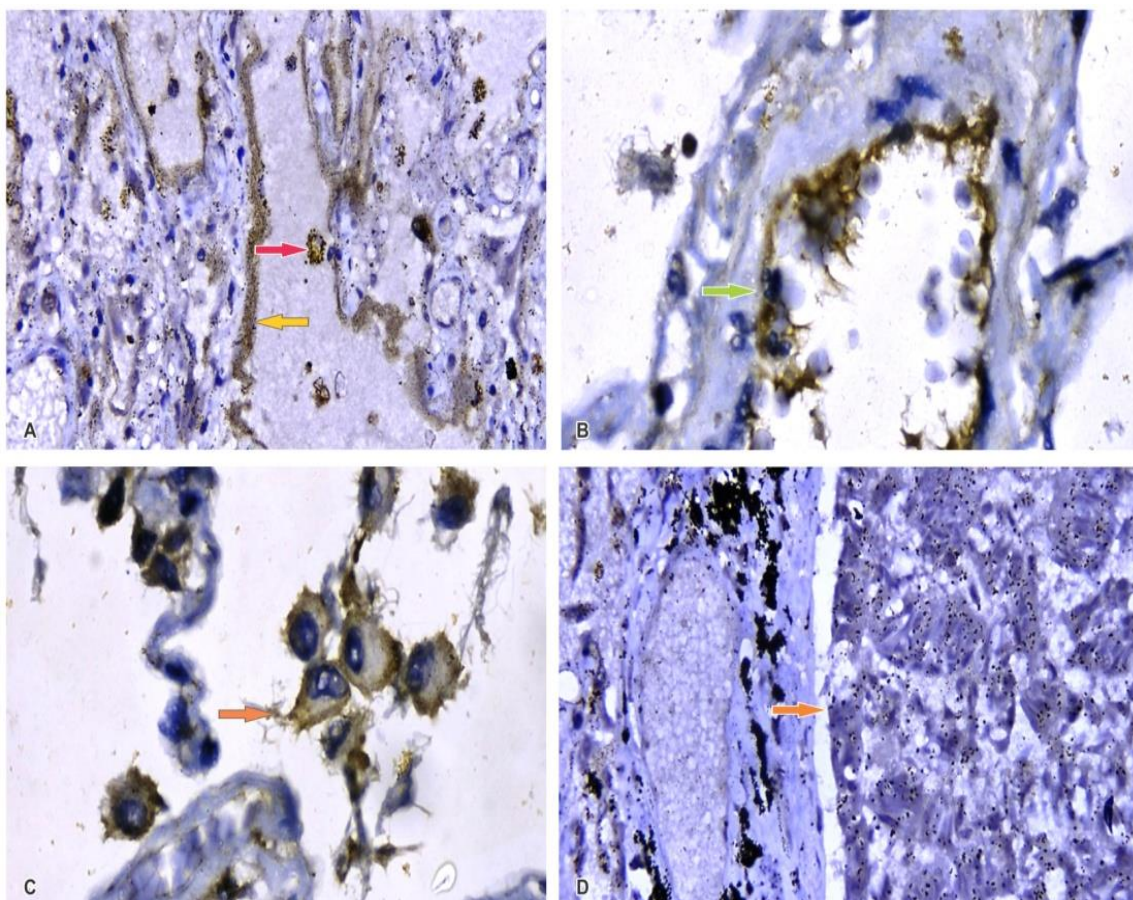
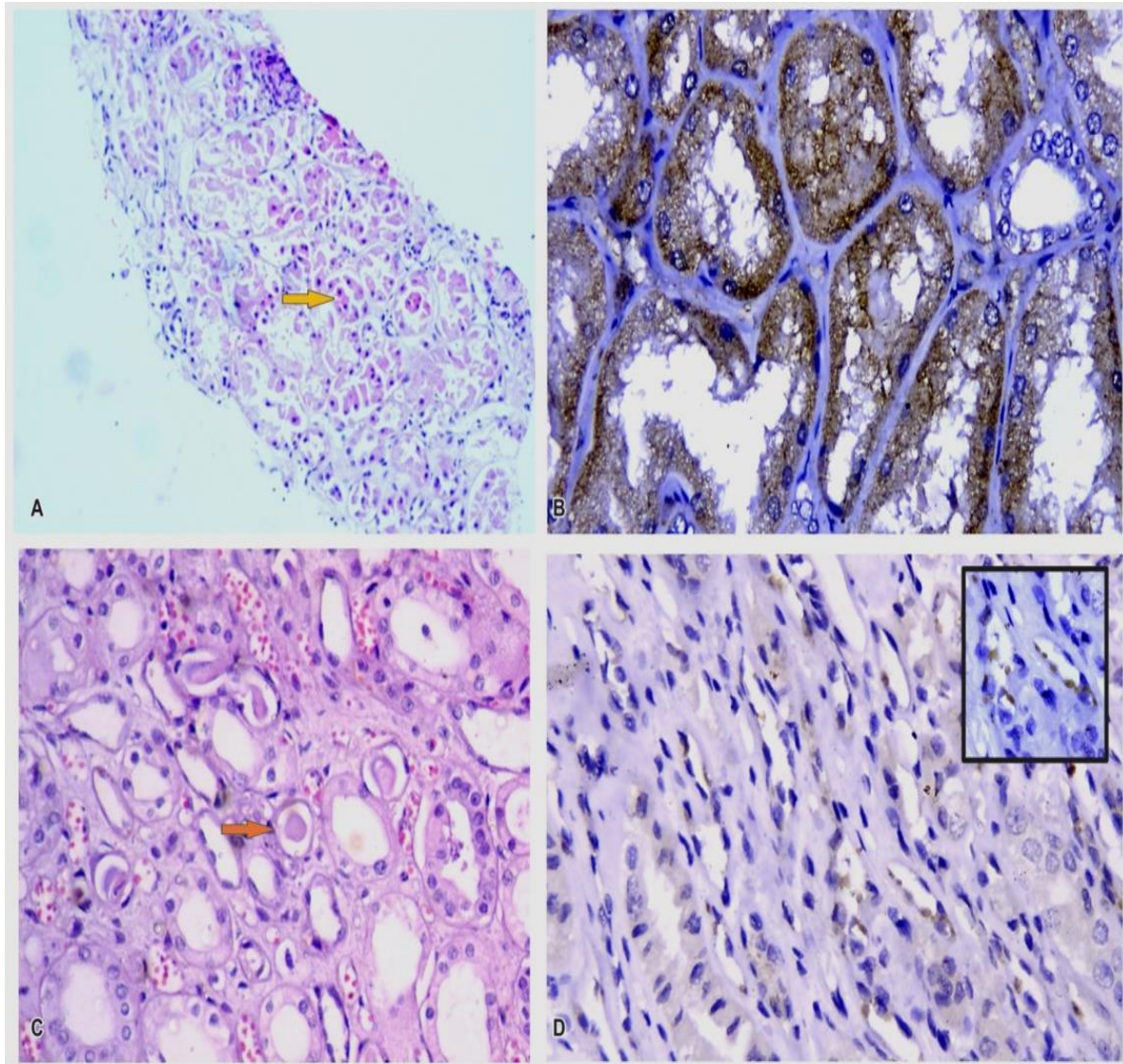


**Figure 5: IHC Staining of Viral particles for SARS CoV 2 in Lung tissue.**



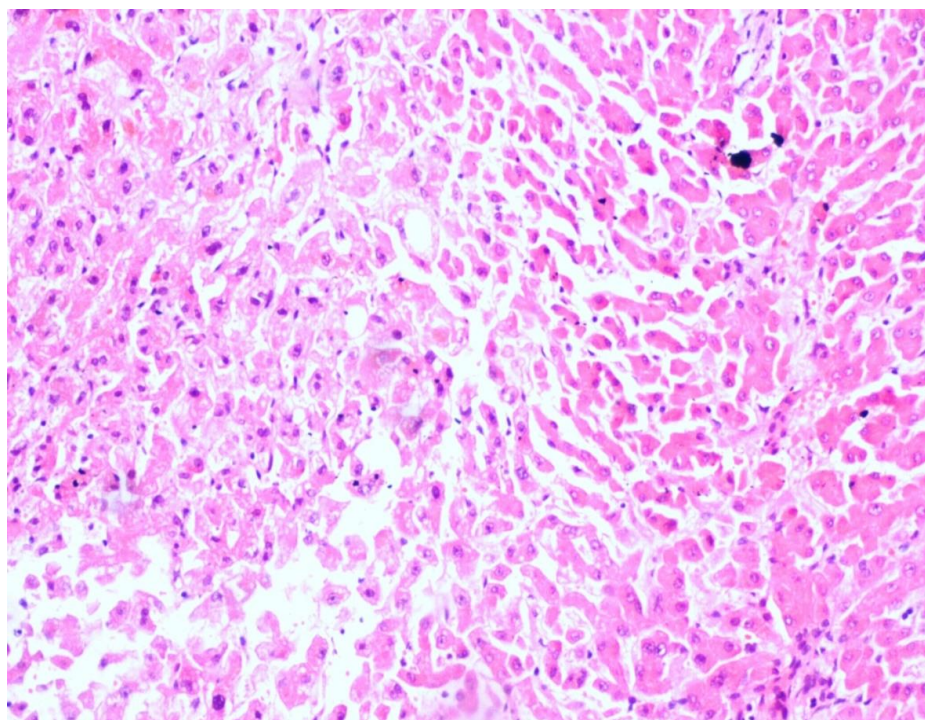
**[A]:** Show Lung tissue showing positive staining in the hyaline membrane and pneumocytes 20x. **[B]:** Lung tissue showing positive staining in the Bronchial epithelial cells,20x. **[C]:** Lung tissue showing positive staining in the detached pneumocytes IHC stain 40x. **[D]:** Lung tissue showing positive staining in the endothelial cells lining the blood vessels, 40x.

**Figure 6: Shows Histopathological and IHC for SARS Co V2 viral particles in Kidney tissue.**

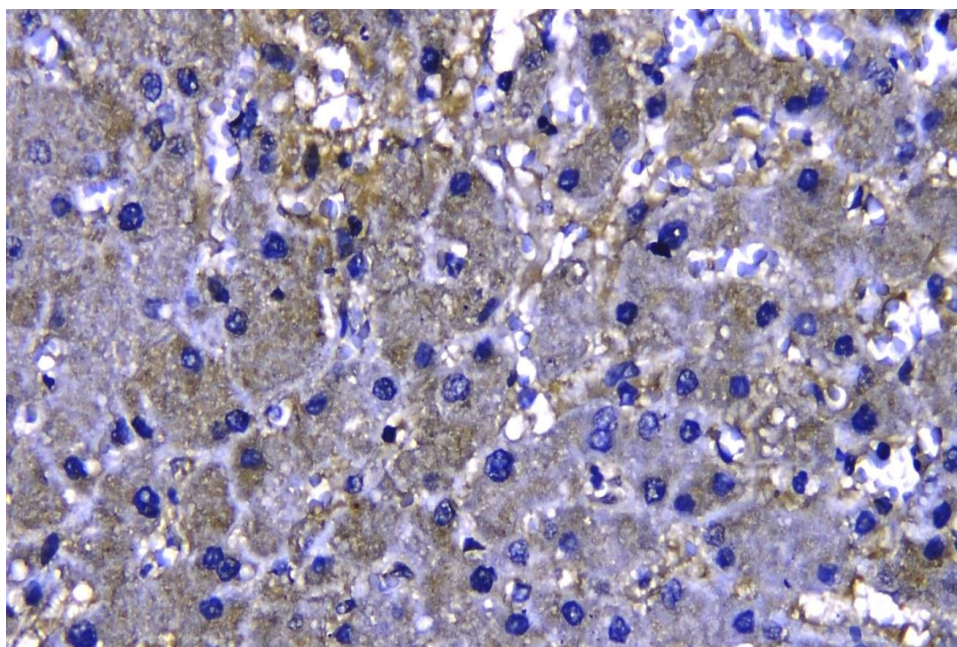


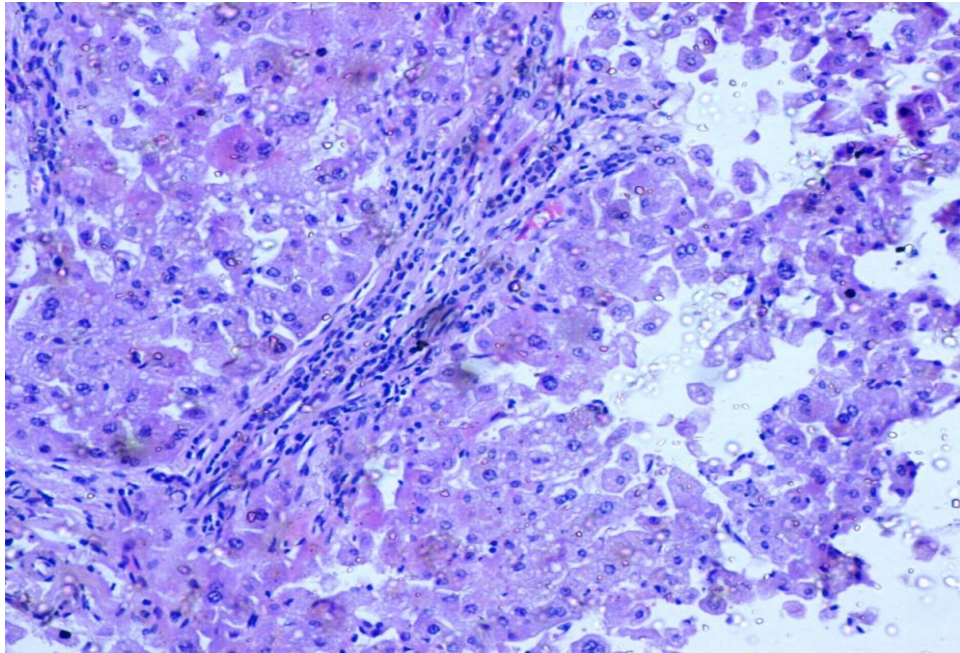
**[A]:** Kidney tissue with features of damage to tubular epithelial cells, enlargement and detached from basement membrane H&E,20X. **[B]:** Kidney tissue showing positive staining in the tubular epithelial cells, 40x. **[C]:** Kidney tissue with features of microthrombi in the small blood vessels, 40X. **[D]:** Kidney tissue showing positive staining in the endothelial cells, 20x.

**Figure 7: Shows Liver tissue with features of damage to Hepatocytes with focal necrosis, H&E,10X.**



**Figure 8: Liver tissue showing positive staining in the hepatocytes by SARS Co V 2 virus, 40x.**



**Figure 9: Shows liver tissue with nuclear inclusions H&E, 20X.****DISCUSSION:**

The COVID-19 pandemic caused by severe acute respiratory distress syndrome-corona virus 2 (SARS CoV2) has recorded a high mortality rate in India of approximately 2.8% with some places showing even higher mortality rates. [1]

The presence of co-morbidities is significantly associated with more severe manifestations, death, and histopathological changes as seen on autopsy.[2]

The histological examination in COVID-19 deaths has been limited both due to the infectivity of the deceased bodies and strict guidelines that need to be followed for opening the bodies. Non-availability of a negative pressure chamber was a major limitation for conducting full covid autopsies.

In the present study, the tissues were obtained using minimally invasive core biopsy needle guns 18 gauge.

Histopathological findings of lungs in COVID-19 deaths are characterized by acute lung injury as seen in 19 cases (95) % in the present study. The lung biopsies showed a spectrum of lesions with some areas showing severe damage and others showing mild congestion due to the nodular and patchy involvement of the lungs. The severity of damage also varied from alveoli to alveoli giving varied histological pictures in different areas in the same patient. The core biopsy tissue obtained from the adjacent uninvolved area may not show any significant pathology. Kligerman et al have described that lungs show a geographic distribution of

involvement seen as ground glass opacities in the CT scans with normal intervening areas.[3]

Diffuse alveolar damage [DAD] is a predominant histological pattern seen in the lungs in 19 cases (95%) in the present study. DAD is seen in cases of severe injury and can be classified broadly into 2 types exudative and proliferative types based on the duration of injury following SARS-CoV-2 infection [3].

The exudative type is seen in the first week following the SARS-CoV-2 infection. As the virus enters the nasal cavity, it binds to the ciliated epithelial cells, expressing ACE2 receptors on them. The virus then starts replicating in these cells and can be detected by nasal swabs. Although the viral burden is low it is infective at this stage. A rise in mucosal CXCL-10 levels and the  $\beta$  and  $\lambda$  interferon levels restrict the infection to upper airways in about 80% of the patients.[4]

The virus enters the cells by binding activated spike protein with the cell containing ACE2 receptors or DC-SIGN integrin molecules. ACE2 receptors are present on type-II pneumocytes, respiratory epithelium, and vascular endothelial cells whereas the integrin molecules are present on the dendritic cells and alveolar macrophages.[5]

The SARS-CoV-2 enters the type 2 pneumocytes, multiplies, and brings about cell death, the release of virions which in turn infects more pneumocytes. These virally infected pneumocytes show the cytopathic changes seen on light microscopy with features of cellular enlargement containing abundant granular eosinophilic cytoplasm, and enlarged nuclei with prominent nucleoli as seen in 14 cases (70%) in our study.

These virus-infected pneumocytes later get detached from the alveolar basement membrane and are seen lying in the alveolar lumen. Damage to the alveolar epithelium is followed by the proliferation of type 2 pneumocytes to repair the damage. On histopathology, they are seen as regenerating pneumocytes with enlarged cell size, an increase in the number of pneumocytes per alveoli, and the presence of multi-nucleated pneumocytes. These changes were noted in 10 cases(50%) in our study. [6] Detachment of damaged and dead alveolar pneumocytes forms the pathway for alveolar damage and Acute respiratory distress syndrome(ARDS) by the leakage of plasma protein-rich fluid into the alveolar space forming hyaline membranes.[6] The hyaline membrane is seen as homogenous eosinophilic material seen plastered against the alveolar wall and alveolar ducts. The hyaline membrane is composed of cellular debris, plasma proteins, and surfactant as seen in 12 of our cases (60%). In the area of hyaline membrane formation the alveolar wall gets denuded of lining epithelial cells and the basement membrane is exposed. [7] Hyaline membrane formation in the alveolar space leads to an increase in the thickness of the alveolar septae and reduces oxygen perfusion causing hypoxia.

The SARS-CoV infection brings about apoptosis of the pneumocytes which are later engulfed by the macrophages[8]. Macrophage recruitment follows the hyaline membrane formation. Macrophages engulf the dead pneumocytes leading to macrophage activation and release of proteases and other cytokines like TGF  $\beta$ , C-TGF, PDGF, IL-1 $\alpha$ , IL-8, and EGF-1 leading to the cytokine storm which is commonly seen in SARS CoV infection. [ 8,5]

The proliferative phase of DAD is seen in the 2nd week of SARS-CoV-2 infection accounting for 13 cases (65%) in the present study. Alveoli with alveolar septae showed fibroblastic proliferation in 13 cases (65%). Both phases of DAD are not strictly sequential and a great deal of overlap is seen between the two phases histologically.[8]The proliferative phase of SARS-CoV-2 infection is mediated by cytokines and is the result of the cytokine storm. TGF  $\beta$  is proposed to be the most important mediator of this cytokine storm along with other cytokines. The proliferative phase of DAD characterized by fibroblastic and vascular proliferation is brought about by the raised TGF  $\beta$  levels.

The integrity of the epithelial and endothelial basement membrane is the key determinant of whether the injured lung tissue returns to normal or is replaced by fixed fibrous tissue. If the basement membrane is intact, the hyaline membrane is removed by the fibrinolytic system, and the normal architecture is reestablished by re-epithelialization and re-endothelialization. Intraluminal fibroblastic proliferation may occur which is remodeled into the interstitium. [9] When the injury damages the integrity of the BM the alveoli collapse and the BM

fuse, fibroblastic activation persists and the formation of organizing fibroblastic tissue progresses to fibrosis seen frequently in the lung tissue of SARS CoV 2 infection.[5]

Along with fibroblastic proliferation, the presence of endothelial proliferation was a common finding seen in 13 cases (65%) in our study.

Angiogenesis of 2 types has been described in the alveolar wall of SARS CoV2 infection which includes sprouting angiogenesis and intussusceptive angiogenesis. Sprouting angiogenesis is the normal budding of endothelium seen in reparative tissues. Intussusceptive angiogenesis is a rapid process of intravascular septation that produces two lumens. This type of inflammation-induced angiogenesis is usually seen in malignancies and inflammatory diseases[9,10].

A study by M Ackerman of examination of the microvascular architecture of lungs from patients of COVID -19 using scanning electron microscopy and microvascular corrosion casting showed distorted vascularity, structurally distorted capillaries, sudden changes in caliber and presence of intussusceptive pillars within the capillaries in the lungs[9].

The chronic phase of SARS Co V 2 infection leads to end-stage fibrosis which is seen in a subset of patients with a longer course of disease of more than 2 -4 weeks duration[7]. It is seen in 1 -6 % of the cases. Early in the disease patchy interstitial fibrosis is seen which progress to diffuse interstitial fibrosis [3].

Acute tubular injury (ATI) was the most frequent finding noted in the kidneys of SARS-CoV-2 infection. 17 out of 20 cases (85%) showed ATI with features of damage and detachment of tubular epithelial cells and acute tubular necrosis. Similar kidney findings have been described by Minami et al.[11] ATI have been reported in kidneys of SARS-CoV 2 infection in the range of 37 to 68 % by various authors.[12] . AKI is associated clinically with increased serum creatinine levels more than 1.5 times the baseline and urinary findings of proteinuria and hematuria.[10]

Mechanisms of ATI in covid-19 are multifactorial and various possibilities are explained. Coagulation disorders associated with covid 19 infection show the presence of fibrin microthrombi leading to tubular ischemia and AKI. Direct invasion of the tubular epithelial cells by the SARS CoV2 virus as proved by a few studies on Electron microscopy and IHC of kidney tissue has demonstrated the presence of few viral particles in tubular epithelial cells. Tubular epithelial cells are known to express ACE 2 receptors making them susceptible to infection. Direct infection from the circulating T lymphocytes has been suggested as a mode of infection.[11]

Fibrin microthrombi in the small blood vessels of the kidney was seen in 75% of cases in the present study.

The liver showed the presence of damage in the hepatocytes surrounding the central vein in 7 cases (35%). The degree of damage varied from ballooning degeneration of the hepatocytes to hemorrhagic necrosis. The study of 14 cases by Benjamin et al on the liver, showed 4 cases with centrilobular necrosis suggestive of hypoperfusion injury. Mild portal lymphocytic infiltration was seen in 95% of the cases in our study which correlated with the study by Benjamin et al [12].

Derangement of the coagulation system is a significant finding in severe SARS-CoV-2 infection with increased Fibrin degradation products (FDP) levels noted in most of the cases. On histopathology presence of microthrombi in various organs is a common finding noted in autopsy studies by various authors. The formation of thrombi in both small and large blood vessels in the lungs, liver, and kidneys has been observed. In the present study, 2 cases showed microthrombi in the lung tissue (10%) and 15 cases (75%) in kidney tissues.

Thrombotic microangiopathy is the feature of COVID-19 coagulopathy with the presence of platelet thrombi in microvasculature causing impaired organ function in various organs. Hemorrhagic complications being less common in COVID -19 coagulopathy is a distinct type of DIC. [13]

Studies on the cellular tropism of the SARCoV-2 have demonstrated viral particles in tissues by various methods such as IHC, FISH, ISH, and Electron microscopy. Genome sequencing and RT-PCR studies have been used to demonstrate the presence of viral genomes in various tissues.

In the present study, Immunohistochemistry staining with SARSCoV-2 antibodies of lung, liver, and kidney tissues of the COVID-19 deaths showed the presence of viral particles in all the organs. The viral particles were demonstrated in both intracellular and extracellular compartments in the lung tissue and were as predominantly intra-cellular in the kidney and liver tissues.

IHC staining of the lung tissues showed positivity for viral particles in all the cases (100%). The alveolar pneumocytes showed the presence of viral particles in all the cases and were the ones to be most intensely stained suggesting they were the cells with the maximum viral particles. The pneumocytes were seen lining the alveoli and detached ones were seen in the alveolar lumen along with the alveolar fluid and debris. The intensity of staining of pneumocytes varied from case to case. Bronchial lining epithelial cells, endothelial cells, and macrophages showed the presence of viral particles in a few cases (20%) with a lesser degree of staining intensity. Extracellular viral particles were observed in the hyaline membrane lining the alveoli in 90% of the cases and alveolar exudates.

In the study of tropism for SARSCoV-2 by ISH with N gene and S gene probes by Bhatnagar et al, the SARSCoV-2 RNA was observed in the hyaline

membrane, intra-alveolar cells, alveolar macrophages, sloughed pneumocytes and bronchial epithelium of the lung tissue similar to the IHC findings of the present study. Genome sequencing of SARSCov2 virus from FFPE detected the presence of viral genome was detected in all the FFPE blocks of lung tissue using RT-Qpcr targeting E gene. [14]

A study by Jennifer L Sauter et al of the detection of viral RNA by NGS and IHC in lung tissue of SARS-CoV patients revealed the presence of a higher number of viral particles in the early acute phase of DAD compared to the cases in the late organizing phase of more than 10 days following infection. [15]

A study by Bhatnagar et al detected the presence of the virus by RT-PCR in multiple organs such as the heart, kidney, liver, brain, small intestine, colon, spleen, and pancreas. [16]

The present study IHC study for kidney tropism of SARS-COV-2 infection detected the presence of viral particles in the tubular epithelial cells and endothelial cells. Kidney tissue showed positivity for viral markers in tubular epithelial cells in 70% of cases, and endothelial cells in 50 % of cases. The intensity of staining was observed to be variable among cases. The rate of positivity for the virus and the intensity (viral load) were lower in comparison to the lungs. In the endothelial cells, the intensity of staining for viral particles was found to be very low.

Kidney complications are relatively common and acute kidney injury [AKI] is a life-threatening complication in patients with COVID -19 and is seen in 0.5 to 7% of cases and 2.9 -23% in ICU. Transmission electron microscopy studies have detected the presence of viral particles in the tubular epithelial cells and podocytes of the kidney providing evidence of direct renal infection occurring in the setting of AKI in COVID-19 [17][18].

IHC study for kidney tropism of SARS-COV-2 infection detected the presence of viral particles in the tubular epithelial cells has suggested the possibility of viral nephropathy. ACE2 receptors have been known to be expressed in the brush border of tubular epithelial cells, therefore, explaining the tropism for the virus. [12]

Liver tissue on IHC demonstrated the presence of viral particles in the hepatocytes in 40% of cases. The number of cases was positive and the viral load was very low in comparison to the lungs and kidney tissues. In a study by Yevgen Chormenkyy et al, RTPCR of liver tissue in SARSCOV-2 infection showed positivity for the viral genome in 44% of cases. [19]

Endothelial cells have been detected to be positive by IHC in the lung and kidney tissues in the present study. IHC and EM studies on skin lesions in SARSCOV2 infection have demonstrated the presence of viral particles in Endothelial cells. [21] Histologically blood vessels showed endothelial

swelling, endothelitis, fibrinoid necrosis, and thrombus formation.[22]

In situ hybridization study by Massot et al demonstrated viral particles in endothelial cells of multiple organs such brain, kidney, liver, and lungs. [23]

Transmission electron microscopy of the endothelium demonstrated the presence of intracellular SARS CoV in the endothelial cells. [9] and ACE2 receptors are expressed on endothelial cells.[24] A multiplex analysis of angiogenesis-related gene expression examining 323 genes revealed that a total 69 of angiogenesis-related genes were differently regulated in the COVID-19 group responsible for the vascular proliferation seen in Covid 19 infection.[8]

### CONCLUSION:

Lung, liver, and kidney tissues showed the presence of distinctive histopathological changes on tissue microscopy. IHC with SARS Cov2 Virus antibodies for Cellular tropism in Lung tissue, viral particles were seen Intracellularly in pneumocytes, endothelial cells, bronchial epithelial cells, fibroblast and extracellular in Hyaline membrane and alveolar exudates. Kidney tissue in Tubular epithelial cells and endothelial cells. Hepatocytes and bile duct epithelium in Liver tissue. On IHC staining for the virus, the viral load of SARS Co V2 was found to be varied from case to case. The density of the viral load was highest in the lung and lower in the kidney and least in the liver.

### REFERENCES

- Chaubey G. Coronavirus (SARS-CoV-2) and Mortality Rate in India: The Winning Edge. *Front Public Heal.* 2020;8(July):1–5. doi: 10.3389/fpubh.2020.00397.
- Biswas M, Rahaman S, Biswas TK, Haque Z, Ibrahim B. Association of Sex, Age, and Comorbidities with Mortality in COVID-19 Patients: A Systematic Review and Meta-Analysis. *Intervirology.* 2021;64(1):36–47. doi: 10.1159/000512592.
- Kligerman SJ, Franks TJ, Galvin JR. From the Radiologic Pathology Archives: Organization and fibrosis as a response to lung injury in diffuse alveolar damage, organizing pneumonia, and acute fibrinous and organizing pneumonia. *Radiographics.* 2013;33(7):1951–75. doi: 10.1148/rg.337130057.
- O'Sullivan MJ, Mitchel JA, Mwase C, McGill M, Kanki P, Park JA. In well-differentiated primary human bronchial epithelial cells, TGF- $\beta$ 1 and TGF- $\beta$ 2 induce expression of furin. *Am J Physiol - Lung Cell Mol Physiol.* 2021;320(2):L246–53. In well-differentiated primary human bronchial epithelial cells, TGF- $\beta$ 1 and TGF- $\beta$ 2 induce expression of furin. | *Am J Physiol Lung Cell Mol Physiol*;320(2): L246-L253, 2021 02 01. | MEDLINE (bvsalud.org)
- Ingrid Carvacho, Matthias Piesche. RGD-binding integrins and TGF-beta in SARS-CoV-2 infections - novel targets to treat COVID-19 patients?. *Clinical and Translational immunology.* 2021;10(3):e1240. doi: 10.1002/cti2.1240.
- Abourida Y, Rebahi H, Chichou H, Fenane H, Msougar Y, Fakhri A, et al. What Open-Lung Biopsy Teaches Us about ARDS in COVID-19 Patients: Mechanisms, Pathology, and Therapeutic Implications. *Biomed Res Int.* 2020;2020. doi: 10.1155/2020/2909673.
- Hariri LP, North CM, Shih AR, Israel RA, Maley JH, Villalba JA, et al. Lung Histopathology in Coronavirus Disease 2019 as Compared With Severe Acute Respiratory Syndrome and H1N1 Influenza: A Systematic Review. *Chest.* 2021;159(1):73–84. doi: 10.1016/j.chest.2020.09.259.
- WanJun Chen. A potential treatment of COVID-19 with TGF-beta blockade. *Int J Biol Sci* 2020;16(11):1954-1955. doi: 10.7150/ijbs.46891
- Ackermann M, Verleden SE, Kuehnel M, Haverich A, Welte T, Laenger F, et al. Pulmonary Vascular Endothelialitis, Thrombosis, and Angiogenesis in Covid-19. *N Engl J Med.* 2020;383(2):120–8. doi: 10.1056/NEJMoa2015432
- Minami T, Iwata Y, Wada T. Renal complications in coronavirus disease 2019: a systematic review. *Inflamm Regen.* 2020;40(1). 12. Renal complications in coronavirus disease 2019: a systematic review | Inflammation and Regeneration | Full Text (biomedcentral.com)
- Santoriello D, Khairallah P, Bomback AS, Xu K, Kudose S, Batal I, et al. Postmortem Kidney Pathology Findings in Patients with COVID-19. *J Am Soc Nephrol.* 2020;31(9):2158–67. doi: 10.1681/ASN.2020050744
- Bradley BT, Maioli H, Johnston R, Chaudhry I, Fink SL, Xu H, et al. Histopathology and ultrastructural findings of fatal COVID-19 infections in Washington State: a case series. *Lancet [Internet].* 2020;396(10247):320–32. doi: 10.1016/S0140-6736(20)31305-2
- Marcel Levi, Toshiaki Iba. COVID-19 coagulopathy: is it disseminated intravascular coagulation? . *Intern Emerg Med.* 2021;16(2):309-312. doi: 10.1007/s11739-020-02601-y.
- Van Campenhout C, De Mendonça R, Alexiou B, De Clercq S, Racu ML, Royer-Chardon C, Rusu S, Van Eycken M, Artesi M, Durkin K, Mardulyn P, Bours V, Decaestecker C, Rimmelink M, Salmon I, D'Haene N. Severe Acute Respiratory Syndrome Coronavirus 2 (SARS-CoV-2) Genome Sequencing from Post-Mortem Formalin-Fixed, Paraffin-Embedded Lung Tissues. *J MolDiagn.* 2021 Sep;23(9):1065-1077. doi: 10.1016/j.jmoldx.2021.05.016. Epub 2021 Jun 18. PMID: 34153515; PMCID: PMC8219372
- Sauter JL, Baine MK, Butnor KJ, Buonocore DJ, Chang JC, Jungbluth AA, Szabolcs MJ, Morjaria S, Mount SL, Rekhtman N, Selbs E, Sheng ZM, Xiao Y, Kleiner DE, Pittaluga S, Taubenberger JK, Rapkiewicz AV, Travis WD. Insights into pathogenesis of fatal COVID-19 pneumonia from histopathology with immunohistochemical and viral RNA studies. *Histopathology.* 2020 Dec;77(6):915-925. doi: 10.1111/his.14201. Epub 2020 Oct 16. PMID: 32614086; PMCID: PMC7361244.
- Bhatnagar J, Gary J, Reagan-Steiner S, Estetter LB, Tong S, Tao Y, Denison AM, Lee E, DeLeon-Carnes M, Li Y, Uehara A, Paden CR, Leitgeb B, Uyeki TM, Martinez RB, Ritter JM, Paddock CD, Shieh WJ, Zaki SR. Evidence of Severe Acute Respiratory Syndrome Coronavirus 2 Replication and Tropism in the Lungs, Airways, and Vascular Endothelium of Patients With

- Fatal Coronavirus Disease 2019: An Autopsy Case Series. *J Infect Dis.* 2021 Mar 3;223(5):752-764. doi: 10.1093/infdis/jiab039. PMID: 33502471; PMCID: PMC7928839.
17. T. Minami, Iwata, Y. & Wada, T. Renal complications in coronavirus disease 2019: a systematic review. *InflammRegener* 40, 31 (2020).<https://doi.org/10.1186/s41232-020-00140-9>
  18. Farkash EA, Wilson AM, Jentzen JM. Ultrastructural Evidence for Direct Renal Infection with SARS-CoV-2. *J Am SocNephrol.* 2020 Aug;31(8):1683-1687. doi: 10.1681/ASN.2020040432. Epub 2020 May 5. Erratum in: *J Am SocNephrol.* 2020 Oct;31(10):2494. PMID: 32371536; PMCID: PMC7460898.
  19. Chornenkyy Y, Mejia-Bautista M, Brucal M, Blanke T, Dittmann D, Yeldandi A, Boike JR, Lomasney JW, Nayar R, Jennings LJ, Pezhouh MK. Liver Pathology and SARS-CoV-2 Detection in Formalin-Fixed Tissue of Patients With COVID-19. *Am J ClinPathol.* 2021 May 18;155(6):802-814. doi: 10.1093/ajcp/aqab009. PMID: 33914058; PMCID: PMC8135761.
  20. Varga Z, Flammer AJ, Steiger P, Haberecker M, Andermatt R, Zinkernagel AS, Mehra MR, Schuepbach RA, Ruschitzka F, Moch H. Endothelial cell infection and endotheliitis in COVID-19. *Lancet.* 2020 May 2;395(10234):1417-1418. doi: 10.1016/S0140-6736(20)30937-5. Epub 2020 Apr 21. PMID: 32325026; PMCID: PMC7172722.
  21. Colmenero I, Santonja C, Alonso-Riaño M, Noguera-Morel L, Hernández-Martín A, Andina D, Wiesner T, Rodríguez-Peralto JL, Requena L, Torrelo A. SARS-CoV-2 endothelial infection causes COVID-19 chilblains: histopathological, immunohistochemical and ultrastructural study of seven paediatric cases. *Br J Dermatol.* 2020 Oct;183(4):729-737. doi: 10.1111/bjd.19327. Epub 2020 Aug 5. PMID: 32562567; PMCID: PMC7323219
  22. Massoth LR, Desai N, Szabolcs A, Harris CK, Neyaz A, Crotty R, Chebib I, Rivera MN, Sholl LM, Stone JR, Ting DT, Deshpande V. Comparison of RNA In Situ Hybridization and Immunohistochemistry Techniques for the Detection and Localization of SARS-CoV-2 in Human Tissues. *Am J SurgPathol.* 2021 Jan;45(1):14-24. doi: 10.1097/PAS.0000000000001563. PMID: 32826529.
  23. Borczuk AC, Salvatore SP, Seshan SV, Patel SS, Bussel JB, Mostyka M, Elsoukkary S, He B, Del Vecchio C, Fortarezza F, Pezzuto F, Navalesi P, Crisanti A, Fowkes ME, Bryce CH, Calabrese F, Beasley MB. COVID-19 pulmonary pathology: a multi-institutional autopsy cohort from Italy and New York City. *Mod Pathol.* 2020 Nov;33(11):2156-2168. doi: 10.1038/s41379-020-00661-1. Epub 2020 Sep 2. PMID: 32879413; PMCID: PMC7463226.